Dhakshinamoorthy, A.; Alvaro Rodríguez, MM.; Concepción Heydorn, P.; García Gómez, H. (2011). Chemical instability of Cu(3)(BTC)(2) by reaction with thiols. Catalysis Communications. 12(11):1018-1021. doi:10.1016/j.catcom.2011.03.018.

Chemical instability of $Cu_3(BTC)_2$ by reaction with thiols

Amarajothi Dhakshinamoorthy, Mercedes Alvaro, Patricia Concepcion and Hermenegildo Garcia*

Instituto Universitario de Tecnología Química CSIC-UPV and Departamento de Química, Universidad Politécnica de Valencia, Av. De los Naranjos s/n, 46022 Valencia, Spain. Fax: +34 96387 7809; Tel: +34 9638 7807

E-mail: hgarcia@qim.upv.es

Abstract

In contrast to Fe(BTC) (BTC: 1,3,5-benzenetricarboxylate), the crystal structure of $Cu_3(BTC)_2$, a commercial metal organic framework widely used as solid catalyst, collapses when contacted with thiols under mild reaction conditions forming copper nanoparticles.

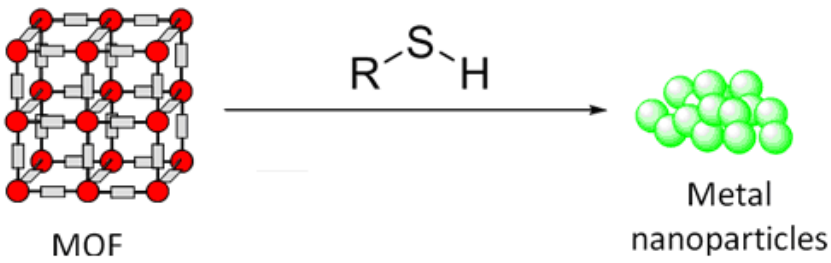

Keywords: $Cu_3(BTC)_2$; copper; metal organic frameworks; thiols; metal nanoparticles.

Introduction

Metal Organic Frameworks (MOFs) have received much current interest in recent years due to their fascinating properties in gas storage[1] and heterogeneous catalysis.[2] Specifically, copper based MOFs namely $Cu_3(BTC)_2$ is one of the best-studied MOFs whose crystal structure has been reported in 1999 and also named as HKUST-1.[3] Since its origin many research works have been carried out with this MOF. For instance, $Cu_3(BTC)_2$ have been used widely as heterogeneous catalysts in acetalization of aldehydes with methanol,[4] quinoline synthesis,[5] α-pinene oxide rearrangement,[6] trimethylsilylazide addition to carbonyl compounds,[7] oxidation of benzylic compounds with *t*-butylhydroperoxide,[8] ring opening of epoxides with methanol,[9] alkylation of amines with dimethyl carbonate,[10] and cycloaddition of phenylacetylene with benzyl azide among other reactions.[11] Considering that the use of MOFs as solid catalysts is a field of growing importance and the ample use of $Cu_3(BTC)_2$ as solid catalysts, it is of interest to delineate the scope and conditions in which this material can be used in catalysis.

Results and Discussion

As a part of our ongoing investigations on the performance of MOFs as heterogeneous catalysts,[4, 9, 10, 12] we were interested in studying the formation of C-S bond through the nucleophilic addition of thiophenol to aryl halides using $Cu_3(BTC)_2$ as a catalyst. It has been already reported in the literature that Cu(II) ions catalyze this particular reaction with very good yield and selectivity.[13] Based on the precedents showing the paralellism between homogeneous metal salts and MOFs,[2, 14] we anticipated that $Cu_3(BTC)_2$ should perform similarly. More specifically, we wanted to carry out the formation of C-S bonds using phenyl sulfide catalyzed by $Cu_3(BTC)_2$ avoiding the formation of diphenyldisulfide that is the product obtained with high yields

when related Fe(BTC) is used as catalyst under aerobic conditions.[12] Scheme 1 summarized the objective of our study.

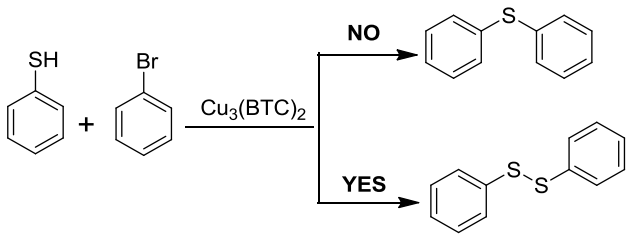

Scheme 1. Attempted cross-coupling to form diphenyldisulfide and observation of thiol oxidation leading to disulfide.

To our surprise, the reaction towards our target C-S product did not occur. The only product observed was the corresponding disulfide in a small amount (18 % conversion) as shown in Scheme 1. On the other hand, 4 % conversion of **2** was noticed towards the formation of 1,2-dithiolane. These low conversions are a consequence of the fact that $Cu_3(BTC)_2$ is not acting a catalyst but as reagent. Thus, we observed a change in the characteristic colour of $Cu_3(BTC)_2$ to form yellow powder as the reaction progressed. This unexpected observation suggests that, in contrast to Fe(BTC) that is stable when catalyzing the formation of disulfides from thiols,[12] $Cu_3(BTC)_2$ was reacting and being converted into a different solid. Due to this result, our aim changed towards determining the chemical reactivity of $Cu_3(BTC)_2$ with thiols. In the present study, we report that the well studied $Cu_3(BTC)_2$ undergoes a transformation in its crystal structure leading to copper nanoparticles. This unexpected transformation has been confirmed by powder X-ray diffraction, infra-red analysis, diffuse reflectance optical spectra, electron spin resonance and electron microscopy. There is currently a debate about the thermal and chemical stability of MOFs compared to zeolites and other related materials with the aim to clarify if they could be used as industrial heterogeneous catalysts. We here report the low chemical stability of $Cu_3(BTC)_2$ towards thiophenol and 1,3-propanedithiol eventhough MOFs are potential candidates

as solid catalysts for liquid phase organic reactions. In the context of the ample use of $Cu_3(BTC)_2$ as catalyst, our aim is to inform about the unsuitability of using $Cu_3(BTC)_2$ in any kind of transformations which involves the use of thiols as one of the component.

To understand the transformation of $Cu_3(BTC)_2$ with thiols, we selected thiophenol (**1**) and 1,3-propanedithiol (2) as reducing agents and treated $Cu_3(BTC)_2$ with them in acetonitrile at 70 ^oC for 1 h. The resulting solids were washed with acetonitrile to remove the corresponding disulfide formed. To determine the changes occurring to the $Cu_3(BTC)_2$ during this treatment with **1** and **2**, we characterized the solid by powder XRD, diffuse reflectance optical spectroscopy (DRS), low temperature *in situ* IR and EPR spectroscopic techniques. The observed results are discussed here.

Figure 1 presents the powder XRD pattern of $Cu_3(BTC)_2$ and the observed material after treatement with **1** and **2**. As it can be seen there the peak pattern and peak intensity characteristic of $Cu_3(BTC)_2$ changes completely and decreases much in intensity when treating $Cu_3(BTC)_2$ either with **1** or **2**, showing that this treatment leads to a radical transformation of the crystal structure. The presence of broad peaks at 2θ 33 and 37 ^{o} suggests the formation of copper metal nanoparticles accompanied by the diffractogram of BTC crystals. The fact that the 33 and 37 peaks are broader when dithiol **2** is used as reagent would indicate that these Cu metal nanoparticles are smaller when $Cu_3(BTC)_2$ is treated with **2** under identical conditions as **1.** This smaller particle size of copper when **2** is used as reducing agent can be rationalized considering that compound **2,** in contrast to thiophenol **1,** has two thiol groups and the S/Cu ratio using **2** is, therefore, twice as high that of compound **1**. Overall, XRD shows that $Cu_3(BTC)_2$ is unstable in the presence of thiols and is transformed by destroying its crystal structure probably into Cu metal and the ligand.

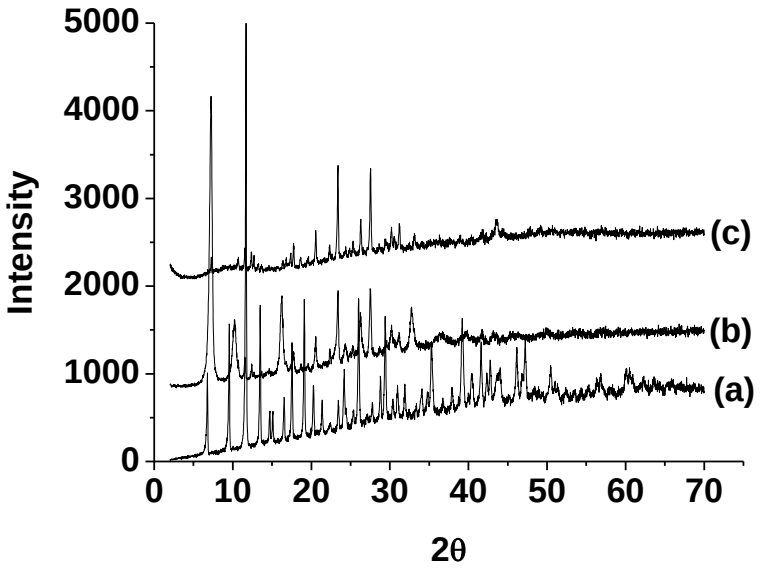

Figure 1. Powder XRD pattern of (a) native $Cu_3(BTC)_2$, (b) $Cu_3(BTC)_2$ treated with **1** and (c) $Cu_3(BTC)_2$ treated with **2** in acetonitrile.

Figure 2 provides DRS of $Cu_3(BTC)_2$ and **1** and **2** treated with $Cu_3(BTC)_2$. The native $Cu_3(BTC)_2$ exhibits two absorption bands around 280 nm and 700 nm. The first one is centred in the aromatic ligand and the latter one is due to the d-d transition of Cu^{2+}. Interestingly, the latter band disappears when $Cu_3(BTC)_2$ is submitted to treatment with any of the two thiols, while the ligand-centred absorption at the shorter wavelength remains. In addition, Figure 2 also shows that the absorption between 200-300 nm characteristic of aromatic linkers has reduced considerably its intensity after treatment of $Cu_3(BTC)_2$ with compound **1** and **2**. The residual absorption in this UV region could probably indicate that some linker or thiol group is still attached to copper nanoparticles.

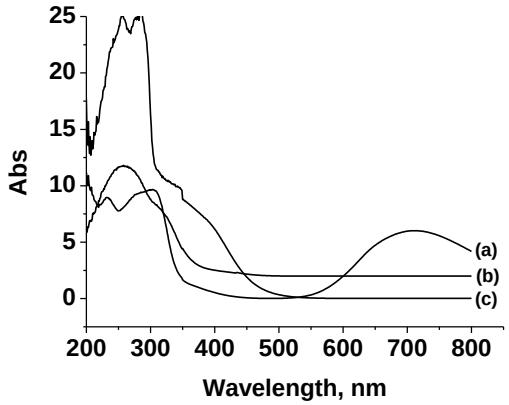

Figure 2. DRS of (a) parent $Cu_3(BTC)_2$ (b) **1** treated with $Cu_3(BTC)_2$ and (c) **2** treated with $Cu_3(BTC)_2$.

From powder XRD it can be concluded that the structure of $Cu_3(BTC)_2$ has completely changed and DRS showed the disappearance of Cu^{2+}. In order to have some information about the nature of copper species present in the samples after treating with **1** and **2**, we subjected them into IR studies using CO as probe molecule. Figures 3, 4 and 5 show the CO region in IR spectroscopy after activation at 150 ^{o}C and low temperature adsorption of CO in native $Cu_3(BTC)_2$ and in the solids resulting of the treatment of $Cu_3(BTC)_2$ with **1** and **2**. Activation was performed at 150 ^{o}C to ensure the complete removal of coadsorbed water inspite that the $Cu_3(BTC)_2$ treatment with thiols was carried out 70 ^{o}C. The absorption band around 2180 to 2171 cm $^{-1}$ clearly suggests the existence of Cu(II) in $Cu_3(BTC)_2$ and also existence of small amount of Cu(I) as evidenced from its absorption band around 2140 cm $^{-1}$ as it has been reported in earlier precedents.[15, 16] On the other hand, Figures 4 and 5 showed the absence of the absorption bands in the above mentioned regions, while the fact that the CO vibration appears below 2100 cm^{-1} is compatible with the interaction of this probe molecule with metallic nanoparticles, suggesting the formation of copper metal species during the reaction of thiols **1** and **2** with $Cu_3(BTC)_2$. Assignment of the FT-IR bands has been

based on the reported CO vibrations for gold nanoparticles.[17-20] For the assignment of CO species, gold is more suitable standard than copper since there is considerable information in the literature about the positon of the CO bonding and also because there is less uncertanity on the oxidation states compared to copper. From these studies it is well established that the more positive is the charge of the center interacting with CO, the higher is the wavelength of the band. CO interacting with metal in the zero oxidation state as those shown in Figures 4 and 5 exhibits vibration peaks below 2100 cm-1 as consequence of electron retrodonation in the antibonding π* orbitals of CO. Hence, these spectroscopic data are compatible with the reduction of Cu (II) to Cu (0) by reaction with **1** and **2**.

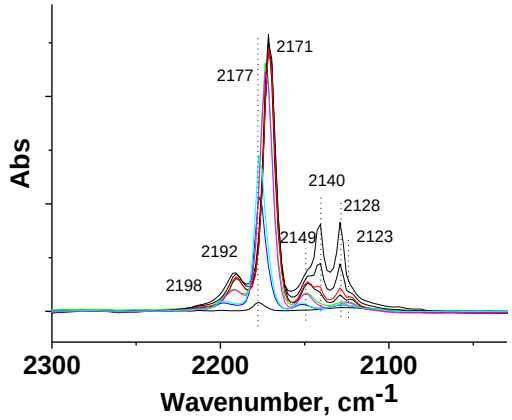

Figure 3. IR spectra of $Cu_3(BTC)_2$ after adsorption of CO as probe molecule. Samples were activated at 150 ^oC for 1 h and adsorption of CO was carried out at -175 ^oC with the dosing from 0 to 13 mbar. The peaks appearing between 2198 and 2171 cm^{-1} correspond to CO interacting with Cu^{2+} ions, while those appearing between 2149 and 2123 cm^{-1} arise from the interaction of CO with Cu^{+} ions.

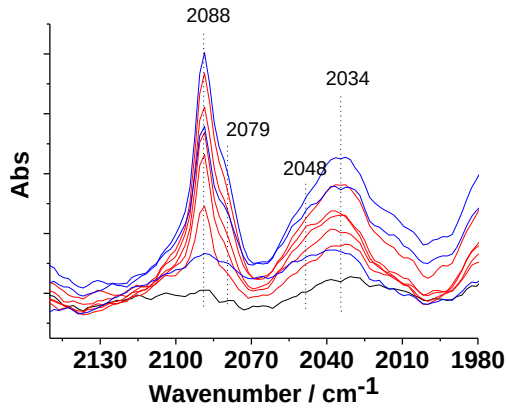

Figure 4. IR spectra of $Cu_3(BTC)_2$ treated with **1** after adsorbing CO as probe molecule. Samples were activated at 150 ^oC for 1 h and adsorption of CO was carried out at -175 ^oC with the dosing from 0 to 13 mbar. The fact that the peak wavenumbers appear below 2100 cm^{-1} indicates that CO is interacting with metal atoms in the zero oxidation state.

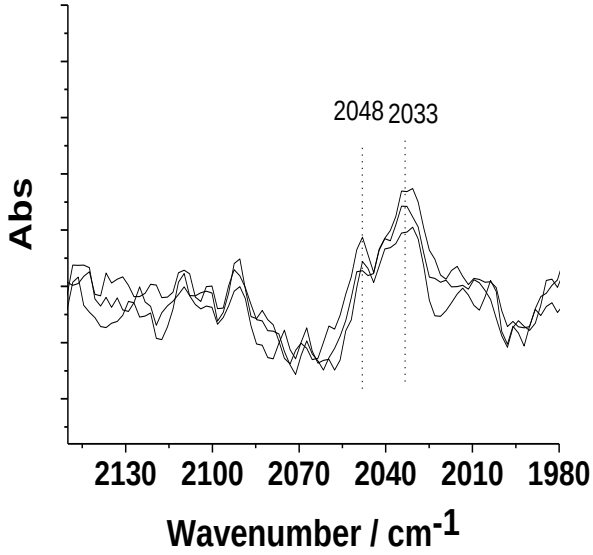

Figure 5. IR spectra of $Cu_3(BTC)_2$ treated with **2** after adsorption of CO as probe molecule. The lower intensity of CO peaks in these FT-IR spectra compared to those shown in Figure 4 is a reflection of the samller particle size of copper nanoparticles when $Cu_3(BTC)_2$, is reduced by dithiol **2** due to the twice as large S/Cu ratio.

The differences between the CO absorption IR spectra resulting after the treatment of $Cu_3(BTC)_2$ with **1** or **2** are again compatible with the smaller particle size of the Cu nanoparticles formed that shifts the CO wavenumber to lower values as the nanoparticle size decreases.

EPR spectra were measured for $Cu_3(BTC)_2$ and **1** and **2** treated with $Cu_3(BTC)_2$. The observed patterns are presented in Figure 5. The native $Cu_3(BTC)_2$ showed the EPR spectrum corresponding to the presence of Cu (II). On the other hand, **1** and **2** treated with $Cu_3(BTC)_2$ showed a decrease in the intensity and a change in the coupling constant of the EPR signal indicating a decrease in the population of EPR active copper species and a change in its coordination. When $Cu_3(BTC)_2$, was treated with **2** (having twice the amount of thiol reducing groups compared to compound **1**), then, the EPR signal completely disappeared. This information agrees with the previous observation from DRS studies.

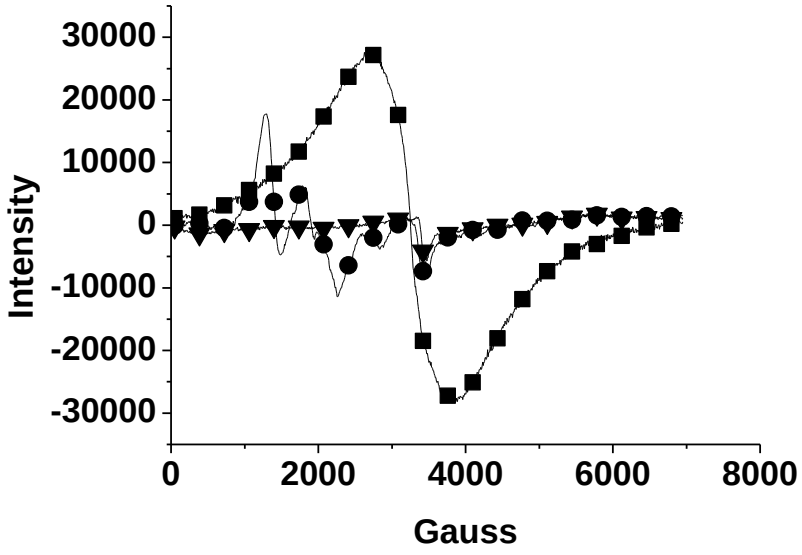

Figure 6. EPR spectra of $Cu_3(BTC)_2$ (square), $Cu_3(BTC)_2$ treated with **1** (circle) and $Cu_3(BTC)_2$ treated with **2** (triangle).

After having the information about the copper species from IR and EPR, we subjected these samples into TEM studies. Figure 7(a) presents the TEM image of native $Cu_3(BTC)_2$ showing the typical organic crystal merged one over other. In contrast, Figures 7(b) and (c) showed complete changes in the morphology of the samples with the clear appearance of metal nanoparticles. As we have commented earlier, $Cu_3(BTC)_2$ treated with **1** showed larger size than with **2**. The average particle size distribution was around 40 and 10 nm for $Cu_3(BTC)_2$ treated with **1** and 2, respectively. The smaller particles obtained when $Cu_3(BTC)_2$ was treated with **2** could be anticipated from lower stretching frequencies observed with CO adsorption in Figure 5.

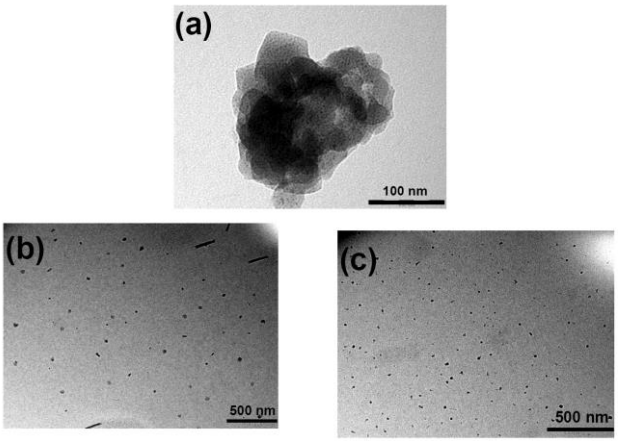

Figure 7. TEM images of (a) $Cu_3(BTC)_2$, (b) and (c) $Cu_3(BTC)_2$ treated with 1 and 2.

Conclusions

The present study highlights that $Cu_3(BTC)_2$ is not compatible with thiols since it becomes transformed into copper metal nanoparticles. Our results are relevant in dileneating the substrates and conditions in which $Cu_3(BTC)_2$, one of the most studied MOF, can be used as heterogeneous catalysts due to its chemical instability against the reagents. In addition, the formation of copper nanoparticles (probably coordinated to phenylthio ligands) could be of potential use in catalysis and this will be reported in due course of time.

Acknowledgements

Financial support by the Spanish DGI (CTQ2009-11587 and CTQ2010-18671) is gratefully acknowledged. Maykel de Miguel is thankful for helping to record TEM images.

Experimental Section

Materials

Basolite C 300 MOF, thiophenol and 1,3-propanedithiol used in the present study was purchased from Sigma Aldrich and used as received. Solvents used in the present study were purchased from Sigma Aldrich.

Characterization techniques

Powder XRD diffraction patterns were recorded in the refraction mode using a Philips X'Pert diffractometer using the CuK_{α} radiation (λ = 1.54178 Å) as the incident beam, PW3050/60 (2 theta) as Goniometer, PW 1774 spinner as sample stage, PW 3011 as detector, incident mask fixed with 10 mm. PW3123/10 for Cu was used as a monochromator. PW3373/00 Cu LFF was used as X-ray tube with power scanning of 45 kV and 40 mA current. The sample powder was loaded into a holder and leveled with a glass slide before mounting it on the sample chamber. The specimens were scanned between 2 to 70 ^{o} with the scan rate of 0.02 /s. ESR spectra were recorded using a Bruker EMX, with the typical settings: frequency 9.80 GHz, sweep width 30.6 G, time constant 80 ms, modulation frequency 100 kHz, modulation width 0.2G, microwave power 200 mW. The size of the nanoparticles was determined by transmission electronmicroscopy (TEM) using a Philips CM300 FEG system with an

operating voltage of 100 kV. TEM samples were prepared by placing microdrops of diamond nanoparticles solution directly onto a copper grid coated with carbon film (200mesh).

Experimental Procedure

To a stirred solution of 0.350 mL of thiophenol in 20 mL of acetonitrile, 500 mg of $Cu_3(BTC)_2$ (sulphur to Cu ratio 1.29 mmol) was charged and the temperature was raised to 70^{o}C under air at atmospheric pressure. This heterogeneous mixture was stirred for 1 h. Then, the pale yellow solid was filtered, washed with acetonitrile (10 mL) in two portions, dried. A silimar procedre was followed with 1,3-propanedithiol under identical conditions as followed for thiophenol. The sulphur to copper ratio (2.66 mmol) in the case of 1,3-propanedithiol was twice that of thiophenol. Similar experiments were carried out at room temperature, as well as 100 ^{o}C observing essentially the same behaviour as that described in the text for 70 ^{o}C.

References

[1] L.J. Murray, M. Dinca and J.R. Long, Chem. Soc. Rev, 38 (2009) 1294.
[2] A. Corma, H. Garcia and F.X. Llabrés i Xamena, Chem. Rev, 110 (2010) 4606.
[3] S.S.-Y. Chui, S.M.-F. Lo, J.P.H. Charmant, A. Guy Orpen and I.D. Williams, Science, 283 (1999) 1148.
[4] A. Dhakshinamoorthy, M. Alvaro and H. Garcia, Adv. Synth. Catal, 352 (2010) 3022.
[5] E. Pérez-Mayoral and J. Čejka, ChemCatChem, (2010) DOI: 10.1002/cctc.201000201.
[6] L. Alaerts, E. Seguin, H. Poelman, F. Thibault-Starzyk, P.A. Jacobs and D.E. De Vos, Chem. Eur. J, 12 (2006) 7353.
[7] K. Schlichte, T. Kratzke and S. Kaskel, Micropor. Mesopor. Mater., 73 (2004) 81.
[8] A. Dhakshinamoorthy, M. Alvaro and H. Garcia, J. Catal, 267 (2009) 1.
[9] A. Dhakshinamoorthy, M. Alvaro and H. Garcia, Chem. Eur. J, 16 (2010) 8530.
[10] A. Dhakshinamoorthy, M. Alvaro and H. Garcia, Appl. Catal. A: Gen, 378 (2010) 19.
[11] I. Luz, F.X. Llabrés i Xamena and A. Corma, J. Catal, 276 (2010) 134.
[12] A. Dhakshinamoorthy, M. Alvaro and H. Garcia, Chem. Commun., 46 (2010) 6476.
[13] S. Bhadra, B. Sreedhar and B.C. Ranu, Adv. Synth. Catal, 351 (2009) 2369.
[14] D. Farrusseng, S. Aguado and C. Pinel, Angew. Chem. Int. Ed, 48 (2009) 7502.
[15] K. Hadjiivanov and H. Knozinger, Phys. Chem. Chem. Phys., 3 (2001) 1132.

[16] N. Drenchev, E. Ivanova, M. Mihaylov and K. Hadjiivanov, Phys. Chem. Chem. Phys., 12 (2010) 6423.
[17] F. Boccuzzi, A. Chiorino and M. Manzoli, Surface Science, 454 (2000) 942.
[18] F. Boccuzzi, A. Chiorino, S. Tsubota and M. Haruta, Journal of Physical Chemistry, 100 (1996) 3625.
[19] S.T. Daniells, A.R. Overweg, M. Makkee and J.A. Moulijn, Journal of Catalysis, 230 (2005) 52.
[20] S. Minico, S. Scire, C. Crisafulli, A.M. Visco and S. Galvagno, Catalysis Letters, 47 (1997) 273.